Environmental Science & Technology

pubs.acs.org/est

Article

Targeted Decomplexation of Metal Complexes for Efficient Metal Recovery by Ozone/Percarbonate

Ying Chen,[⊥] Yi Mu,[⊥] Lei Tian, Ling-Ling Zheng, Yi Mei, Qiu-Ju Xing, Wen Liu, Jian-Ping Zou,* Lixia Yang, Shenglian Luo, and Daishe Wu

Cite This: *Environ. Sci. Technol.* 2023, 57, 5034−5045

Read Online

ACCESS | Metrics & More | Article Recommendations | Supporting Information

ABSTRACT: Traditional methods cannot efficiently recover Cu from Cu(II)−EDTA wastewater and encounter the formation of secondary contaminants. In this study, an ozone/percarbonate (O_3/SPC) process was proposed to efficiently decomplex Cu(II)−EDTA and simultaneously recover Cu. The results demonstrate that the O_3/SPC process achieves 100% recovery of Cu with the corresponding k_{obs} value of 0.103 min^{-1} compared with the typical $^{\bullet}OH$-based O_3/H_2O_2 process (81.2%, 0.042 min^{-1}). The carbonate radical anion ($CO_3^{\bullet-}$) is generated from the O_3/SPC process and carries out the targeted attack of amino groups of Cu(II)−EDTA for decarboxylation and deamination processes, resulting in successive cleavage of Cu−O and Cu−N bonds. In comparison, the $^{\bullet}OH$-based O_3/H_2O_2 process is predominantly responsible for the breakage of Cu−O bonds via decarboxylation and formic acid removal. Moreover, the released Cu(II) can be transformed into stable copper precipitates by employing an endogenous precipitant (CO_3^{2-}), accompanied by toxic-free byproducts in the O_3/SPC process. More importantly, the O_3/SPC process exhibits excellent metal recovery in the treatment of real copper electroplating wastewater and other metal−EDTA complexes. This study provides a promising technology and opens a new avenue for the efficient decomplexation of metal−organic complexes with simultaneous recovery of valuable metal resources.

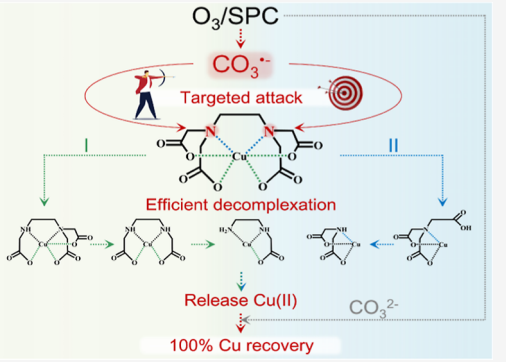

KEYWORDS: *ozone, percarbonate, decomplexation, Cu recovery, carbonate radical anion*

INTRODUCTION

A large amount of metal wastewater containing ethylenediaminetetraacetic acid-chelated copper [Cu(II)−EDTA] was produced from metal smelting, electrolysis, electroplating, and chemical cleaning industries.[1−4] However, traditional chemical precipitation and adsorption processes cannot eliminate Cu(II)−EDTA.[5] Fenton oxidation process reveals its capability in the abatement of Cu(II)−EDTA but faces the problem caused by the secondary solid waste (i.e., iron sludge containing copper ions), thus impeding copper resource for reuse.[6,7] For sustainable industrial development, it is essential to develop feasible treatment processes to remove the Cu−organic complex and recover Cu.

Decomplexation of the Cu−organic complex is a significant step for the recovery of Cu.[8] Currently, a two-step strategy [i.e., preoxidation of EDTA to lose the complexing ability and postprecipitation for free Cu(II)] has become an attractive approach for the Cu recovery from the Cu(II)−EDTA complex.[9,10] Nevertheless, two inherent drawbacks of the two-step strategy induce the low efficiency of Cu recovery, namely, (i) most of the preoxidation processes exhibit low decomplexation rates of Cu(II)−EDTA, which hinder the release of Cu(II)[11] and (ii) the recomplexation between Cu(II) and degradation intermediates of EDTA leads to the formation of stable Cu complexes.[12] To overcome the above-mentioned drawbacks, suitable approaches are devised to achieve the highly efficient decomplexation of Cu(II)−EDTA with simultaneous Cu recovery. Note that the amino groups of EDTA are the critical attack sites for Cu(II)−EDTA decomplexation by active species, which can result in successive cleavage of Cu−organic bonds (i.e., Cu−O and Cu−N bonds).[11,13] Huang et al. found that the chlorine radical ($^{\bullet}Cl$) generated by UV/chlorine facilitated the efficient Cu(II)−EDTA decomplexation with simultaneous Cu recovery at alkaline pH.[14] The phenomenon was mainly ascribed to the high reactivity of $^{\bullet}Cl$ toward the electron-rich amino groups of Cu(II)−EDTA. However, toxic chlorinated byproducts (such as plenty of residual chlorine, chlorinated decomplexation byproducts, dichloroacetic acid, and trichloroacetic acid) would be inevitably generated by reactive chlorine species-mediated advanced oxidation process, which made it

Received: January 9, 2023
Revised: March 2, 2023
Accepted: March 3, 2023
Published: March 14, 2023

https://doi.org/10.1021/acs.est.3c00190
Environ. Sci. Technol. 2023, 57, 5034−5045

inappropriate for the subsequent biological posttreatment.[1,15,16] For break through in achieving toxic-free byproducts, a novel alternative process is desired to carry out the targeted attack on the amino groups for efficient Cu(II)−EDTA decomplexation with simultaneous Cu recovery.

Carbonate radical anion ($CO_3^{\bullet-}$) is an electrophilic reagent, which can react selectively with electron-rich sites of the compounds (such as N-containing moieties) at high reaction rates ($\sim 10^9$ M^{-1} s^{-1}).[17] Besides, the lifetime of $CO_3^{\bullet-}$ is 3 orders of magnitude longer than common radicals (such as hydroxyl radicals ($^{\bullet}OH$) and $^{\bullet}Cl$) in the reaction medium.[18,19] This is because the radical−radical recombination rate of $CO_3^{\bullet-}$ ($k = 2.0 \times 10^7$ M^{-1} s^{-1}) is much slower than those of $^{\bullet}OH$ ($k = 5.5 \times 10^9$ M^{-1} s^{-1}) and $^{\bullet}Cl$ ($k = 8.8 \times 10^7$ M^{-1} s^{-1}) and slower than the recombination reaction rate between $^{\bullet}Cl$ and coexisting chlorate (such as $k^{\bullet}Cl$, $ClO^- = 8.3 \times 10^9$ M^{-1} s^{-1}).[20,21] It can be inferred that $CO_3^{\bullet-}$ would tend to attack the electron-rich amino groups of Cu(II)−EDTA more adequately. It is generally known that carbonate anions (CO_3^{2-}) can react with $^{\bullet}OH$ to generate $CO_3^{\bullet-}$ ($k = 4.2 \times 10^8$ M^{-1} s^{-1}).[22] The existing CO_3^{2-} can also act as an endogenous precipitant to transform Cu(II) into stable copper precipitates, such as $Cu(OH)_2$ ($K_{sp} = 2.2 \times 10^{-20}$), $CuCO_3$ ($K_{sp} = 1.4 \times 10^{-10}$), $CuCO_3{\cdot}Cu(OH)_2$ ($K_{sp} = 1.7 \times 10^{-33}$), and CuO without extra alkali consumption (1).[23−25] Thus, $CO_3^{\bullet-}$-mediated oxidization process is expected to accomplish not only the effective Cu(II)−EDTA decomplexation but also Cu recovery. To date, several studies have reported that the addition of CO_3^{2-} in the $^{\bullet}OH$-based oxidation process would affect the decomplexation efficiency of Cu(II)−EDTA.[8,9,26] However, the performance and mechanism of Cu(II)−EDTA decomplexation by the attack of $CO_3^{\bullet-}$ is still unclear.

$$Cu(II) + OH^- \rightarrow Cu(OH)_2 \quad (1)$$

$$Cu(II) + CO_3^{2-} \rightarrow CuCO_3 \quad (2)$$

$$Cu(II) + CO_3^{2-} + 2H_2O \rightarrow Cu_2(OH)_2CO_3 + 2H^+ \quad (3)$$

$$CuCO_3{\cdot}Cu(OH)_2 + OH^- \rightarrow CuO + CO_3^{2-} + H_2O \quad (4)$$

In this study, we first propose the ozone/percarbonate (O_3/SPC) process for efficient Cu(II)−EDTA decomplexation with simultaneous Cu recovery, which is an economic and environmentally friendly method to generate $CO_3^{\bullet-}$ as the main active species.[27,28] In detail, in comparison to the combination of liquid H_2O_2 and Na_2CO_3, SPC ($Na_2CO_3{\cdot}1.5H_2O_2$) as a solid-phase oxidant has the advantages of longer storage time and superior antiexplosion in the dry environment, as well as lower economic cost for the application.[29] Additionally, many studies have pointed out that SPC and its byproducts have no toxic impact on living organisms, enabling the O_3/SPC process to combine with a subsequent biological process.[30] The performance of Cu(II)−EDTA decomplexation and Cu recovery were systematically investigated in the O_3/SPC process in comparison with the traditional O_3/H_2O_2 process. Density functional theory (DFT) calculations and liquid chromatograph mass spectrometry/mass spectrometry (LC−MS/MS) indicated the different decomplexation pathways of Cu(II)−EDTA in the processes of O_3/SPC and O_3/H_2O_2, confirming the key role of $CO_3^{\bullet-}$ in the decomplexation of Cu(II)−EDTA. The toxicity of the degradation intermediates and products in the O_3/SPC process was discussed. Furthermore, real copper electroplating wastewater and other metal−EDTA complexes were further employed to affirm the practical applicability of the O_3/SPC process. This study illuminates the decomplexation mechanisms of Cu(II)−EDTA in the different advanced oxidation processes and provides a new idea for the development and application of new technologies for the high-efficient treatment of metal complex wastewater.

EXPERIMENTAL SECTION

Chemicals and Reagents. Details of chemicals and reagents used in this study are provided in Text S1 of the Supporting Information.

Experimental Procedures on the Oxidation of Cu(II)−EDTA. All degradation experiments were conducted in a cylindrical glass reactor (volume of 400 mL and 60 mm in diameter) containing 300 mL of 0.1 mM Cu(II)−EDTA stock solution with an initial pH value of 7.0 ± 0.1. The O_3 gas was generated by feeding dry air into the ozone generator (Tonglin EXT-C, Beijing) with a fixed flow rate (100 mL min^{-1}).[31] The O_3/SPC experiment was initiated by turning on the ozone generator and simultaneously adding SPC ($Na_2CO_3{\cdot}1.5H_2O_2$). At regular intervals, 1.5 mL of samples were extracted and filtered through 0.22 μm nylon filter membranes. 0.2 mL of 0.1 M $Na_2S_2O_3$ was immediately added to quench the remaining O_3 gas in the samples. For comparison, the O_3/H_2O_2 process was performed using H_2O_2 in equal molar concentration to the constituents of SPC. Owing to the alkaline and buffering properties of SPC, the pH of the reaction solution would quickly rise to alkaline conditions and remain relatively stable after SPC addition in the O_3/SPC process. The pH values in the processes of ozonation and O_3/H_2O_2 were adjusted to the same alkaline condition as the O_3/SPC process by using 10 M NaOH. The real copper electroplating wastewater was collected from a company in Guangdong Province. The water quality parameters of the real wastewater are shown in Table S1. All degradation experiments were repeated independently three times.

Analytical Methods. Details on the performance evaluation of Cu recovery and total organic carbon (TOC) removal, characterization methods of the precipitate, contribution of active species {electron paramagnetic resonance (EPR) trapping measurement, identification of the inhibitory effect of active species scavenger, and identification of other active species [including Cu(III), Cu(I), and active chlorine]}, determination of Cu(II)−EDTA and its intermediates, toxicity assessment, and electrical energy consumption are shown in Texts S2−S7.

Theoretical Calculation. DFT on electrostatic potential (ESP), Fukui function, and Gibbs free energies (ΔG) were conducted to reveal the discrepancy of active species ($CO_3^{\bullet-}$ and $^{\bullet}OH$) attack on Cu(II)−EDTA. Details of theoretical calculations are presented in Text S8.

RESULTS AND DISCUSSION

Cu Recovery Performance. SPC ($Na_2CO_3{\cdot}1.5H_2O_2$) dosage and O_3 concentration were the key parameters in the O_3/SPC process. As illustrated in Figures S1 and S2, the increase in SPC dosage (0.5−2 mM) and O_3 concentration (0.1−0.3 mM) promoted the recovery of Cu, and the corresponding Cu recovery rate (k_{obs}) exponentially increased.

https://doi.org/10.1021/acs.est.3c00190
Environ. Sci. Technol. 2023, 57, 5034−5045

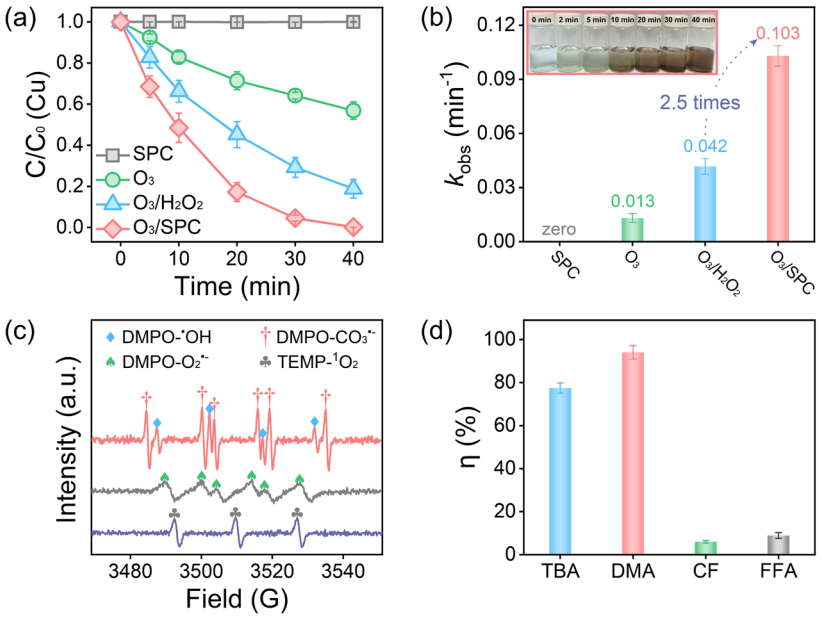

Figure 1. (a) Recovery of Cu and (b) corresponding k_{obs} values in different processes. Inset of (b): change of solution color during the degradation of Cu(II)−EDTA in the O_3/SPC process. (c) EPR spectra of active species in the O_3/SPC process. (d) Inhibitory effect (η) of active species scavengers (TBA for $^{\bullet}OH$, DMA for $CO_3^{\bullet-}$, CF for $O_2^{\bullet-}$, and FFA for $^1O_2$) on the Cu recovery rate in the O_3/SPC process. Experimental conditions: $[Cu(II)-EDTA]_0$ = 0.1 mM, $[O_3]$ = 0.3 mM, $[SPC]_0$ = 2 mM, $[H_2O_2]_0$ = 3 mM, [DMPO] or [TEMP] = 100 mM, [scavenger] = 5 mM, and initial pH = 7.

However, excess SPC (4 mM) and O_3 concentration (0.4 mM) scavenged the generated active species and could not further enhance the recovery rate of Cu.[32,33] Hence, 2 mM SPC and 0.3 mM O_3 were chosen as optimum parameters to achieve 100% Cu recovery in the O_3/SPC process.

To further verify the Cu recovery performance in the O_3/SPC process, the Cu recovery in the SPC alone, ozonation, and O_3/H_2O_2 processes were compared in Figure 1a,b. Considering the alkaline and buffering properties of SPC, the adjustment of the solution pH was conducted during the processes of ozonation and O_3/H_2O_2 (Figure S3). Negligible Cu recovery was observed in the SPC alone process. In the ozonation process, 40.1% of Cu recovery with the corresponding k_{obs} value at 0.013 min^{-1} was achieved. The observation was ascribed to ozone decomposition and associated $^{\bullet}OH$ formation, promoting Cu(II)−EDTA decomplexation (eq 5).[34] As for the O_3/H_2O_2 process, 81.2% of Cu was finally recovered in the same reaction time. The improvement was attributed to an increase in the generation of $^{\bullet}OH$ from the reaction of O_3 and H_2O_2 (eqs 6 and 7), enhancing the release of Cu from Cu(II)−EDTA.[35,36] Note that 100% Cu recovery obtained in the O_3/SPC process was higher than that in the O_3/H_2O_2 process. Besides, the k_{obs} value of Cu recovery in the O_3/SPC process (0.103 min^{-1}) was about 2.5 times that in the O_3/H_2O_2 process (0.042 min^{-1}). These results imply the superiority of the O_3/SPC process over traditional $^{\bullet}OH$-based oxidation processes in terms of Cu recovery from the Cu(II)−EDTA complex.

$$O_3 + OH^- \rightarrow {}^{\bullet}OH + {}^{\bullet}O_3^- \qquad k = (70 \pm 7)\ M^{-1}\ s^{-1} \tag{5}$$

$$H_2O_2 \rightarrow HO_2^- + H^+ \qquad pK_a = 11.62 \tag{6}$$

$$O_3 + HO_2^- \rightarrow {}^{\bullet}OH + O_2 + O_2^{\bullet-} \qquad k = 2.8 \times 10^6\ M^{-1}\ s^{-1} \tag{7}$$

The rapid change of solution color accompanied by the generation of precipitate also validated efficient Cu recovery in the O_3/SPC process (inset Figure 1b). The dark brown precipitate was eventually obtained, which was identified as CuO by the X-ray diffractometer (XRD) pattern (JCPDS no. 80-1916) (Figure S4a). The X-ray photoelectron spectroscopy (XPS) analysis further confirmed that the precipitate contained $CuCO_3$, CuO, and $Cu(OH)_2$ (Figure S4b,c). The TOC removal efficiency was 39.2% in the O_3/SPC process (Figure S5), which was much lower than the Cu recovery efficiency (100%). In comparison, a high level of TOC removal efficiency (62.1%) was accomplished in the O_3/H_2O_2 process, which was only 19.1% lower than the Cu recovery efficiency (81.2%). These findings hinted that the generated active species were favorable to the cleavage of Cu−organic bonds for efficient Cu recovery in the O_3/SPC process rather than complete oxidation of the complexing agent.

Identification of Active Species. To further shed light on the mechanism for Cu recovery in the O_3/SPC process, equal molar concentrations of liquid H_2O_2 and Na_2CO_3 were employed to replace SPC under the same ozonation condition for comparison. As shown in Figure S6, the same tendency of Cu recovery from Cu(II)−EDTA complex was obtained, indicating the reactive species in the O_3/SPC process was on account of the existence of carbonate. Thus, electron paramagnetic resonance (EPR) trapping measurement with the assistance of 5,5-dimethyl-1-pyrroline N-oxide (DMPO) or 2,2,6,6-tetramethylpiperidine (TEMP) as the spin-trapping agent was utilized to detect the generated reactive species in the O_3/SPC process. As shown in Figure 1c, DMPO−$CO_3^{\bullet-}$ (A_N = 15.8 G, A_H = 19.10 G), DMPO−$^{\bullet}OH$ ($A_N = A_H$ = 14.86 G), DMPO−$O_2^{\bullet-}$ (A_N = 13.85 G, A_H = 10.10 G), and TEMP−$^1O_2$ (A_N = 17.32 G) spin adducts were observed in the O_3/SPC process (8).[2,37,38] Subsequently, the quenching experiments using different scavengers were conducted to verify the contributions of these active species in the O_3/SPC

https://doi.org/10.1021/acs.est.3c00190
Environ. Sci. Technol. 2023, 57, 5034−5045

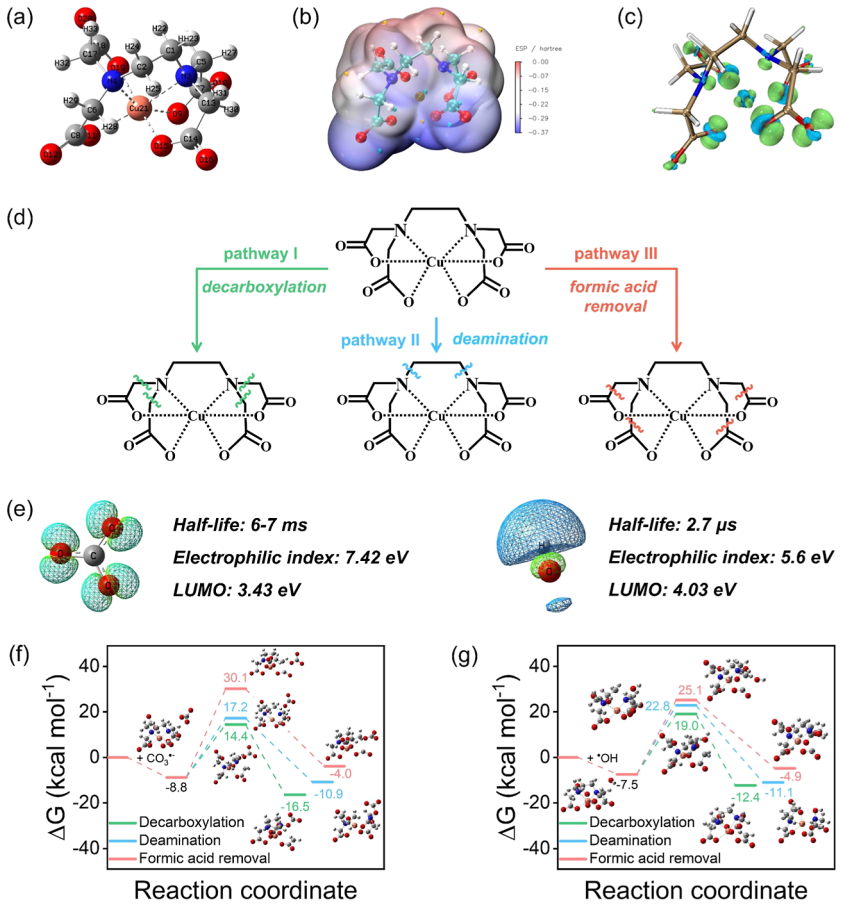

Figure 2. Chemical structure of Cu(II)−EDTA (a). ESP-mapping result (b) and Fukui function isosurface of Cu(II)−EDTA with an isovalue of 0.005 (c). Possible decomplexation pathways of Cu(II)−EDTA by the attack of $CO_3^{\bullet-}$/$^{\bullet}OH$ (d). LUMO orbitals and characteristics of $CO_3^{\bullet-}$ and $^{\bullet}OH$ (e). Profiles of potential energy for reactions of $CO_3^{\bullet-}$ (f) and $^{\bullet}OH$ (g) with Cu(II)−EDTA.

process. As shown in Figure S7a, the Cu recovery efficiency was significantly decreased to 60.5% and 21.3% with the addition of *tert*-butyl alcohol (TBA) and *N*,*N*-dimethylaniline (DMA), respectively.[39] Employing k_{obs} value of Cu recovery as an indicator, the inhibitory effect of DMA on Cu recovery (94.1%) was higher than that of TBA (77.5%) (Figure S7b).[40] This was further confirmed by the quantitative determination of $^{\bullet}OH$ and $CO_3^{\bullet-}$ in the O_3/SPC process, where the concentration of $CO_3^{\bullet-}$ was considerably higher than the concentration of $^{\bullet}OH$ (Figure S8). By contrast, O_3/H_2O_2 possessed significantly higher EPR signals of DMPO−$^{\bullet}OH$ than that in the O_3/SPC process (Figure S9). These results indicated that $CO_3^{\bullet-}$ was derived from $^{\bullet}OH$ in the O_3/SPC process and played a critical role in the Cu(II)−EDTA decomplexation process. In addition, chloroform (CF) and furfuryl alcohol (FFA) exhibited a negligible inhibitory effect on Cu recovery, excluding the contributions of $O_2^{\bullet-}$ and $^1O_2$ in Cu(II)−EDTA decomplexation. It was reported that the generated Cu(II) during the reaction could be involved in the catalytic O_3 or H_2O_2 process to generate more active species, accelerating Cu(II)−EDTA decomplexation (eqs 13 and 14).[41,42] As for the Cu(II) catalytic O_3 process, Cu(III) and $^{\bullet}OH$ could be generated through the one-electron transfer mechanism. Periodate was reported to stabilize Cu(III) to form Cu(III)−periodate complex with a characteristic absorbance at 415 nm.[43] However, no absorbance at this wavelength was observed when periodate was added to the O_3/SPC process (Figure S10), suggesting that the catalytic process of O_3 by Cu(II) did not exist in the O_3/SPC process. Furthermore, Cu(I) was not detected in the O_3/SPC process by using the bathocuproine method (Figure S11), suggesting that the generated Cu(II) did not catalyze H_2O_2.[7] No detection of Cu(I) also ruled out the catalytic process between Cu(I) and O_3 (or H_2O_2) in the O_3/SPC process. Hence, it could be concluded that $CO_3^{\bullet-}$ was the dominant active species for enhanced Cu(II)−EDTA decomplexation in the O_3/SPC process.

$$Na_2CO_3{\cdot}1.5H_2O_2 \rightarrow 2Na^+ + CO_3^{2-} + 1.5H_2O_2 \quad (8)$$

$$CO_3^{2-} + {}^{\bullet}OH \rightarrow CO_3^{\bullet-} + OH^-/H_2O \qquad k = 3.9 \times 10^8\ M^{-1}\ s^{-1} \quad (9)$$

$$^{\bullet}OH + H_2O_2 \rightarrow {}^{\bullet}HO_2 + H_2O \qquad k = 2.7 \times 10^7\ M^{-1}\ s^{-1} \quad (10)$$

$$^{\bullet}HO_2 \leftrightarrow O_2^{\bullet-} + H^+ \qquad pK_a = 4.8 \quad (11)$$

$$^{\bullet}OH + O_2^{\bullet-} \rightarrow {}^1O_2 + OH^- \qquad k = 1.01 \times 10^{10}\ M^{-1}\ s^{-1} \quad (12)$$

$$Cu(II) + H^+ + O_3 \rightarrow Cu(III) + O_2 + {}^{\bullet}OH \quad (13)$$

https://doi.org/10.1021/acs.est.3c00190
Environ. Sci. Technol. 2023, 57, 5034−5045

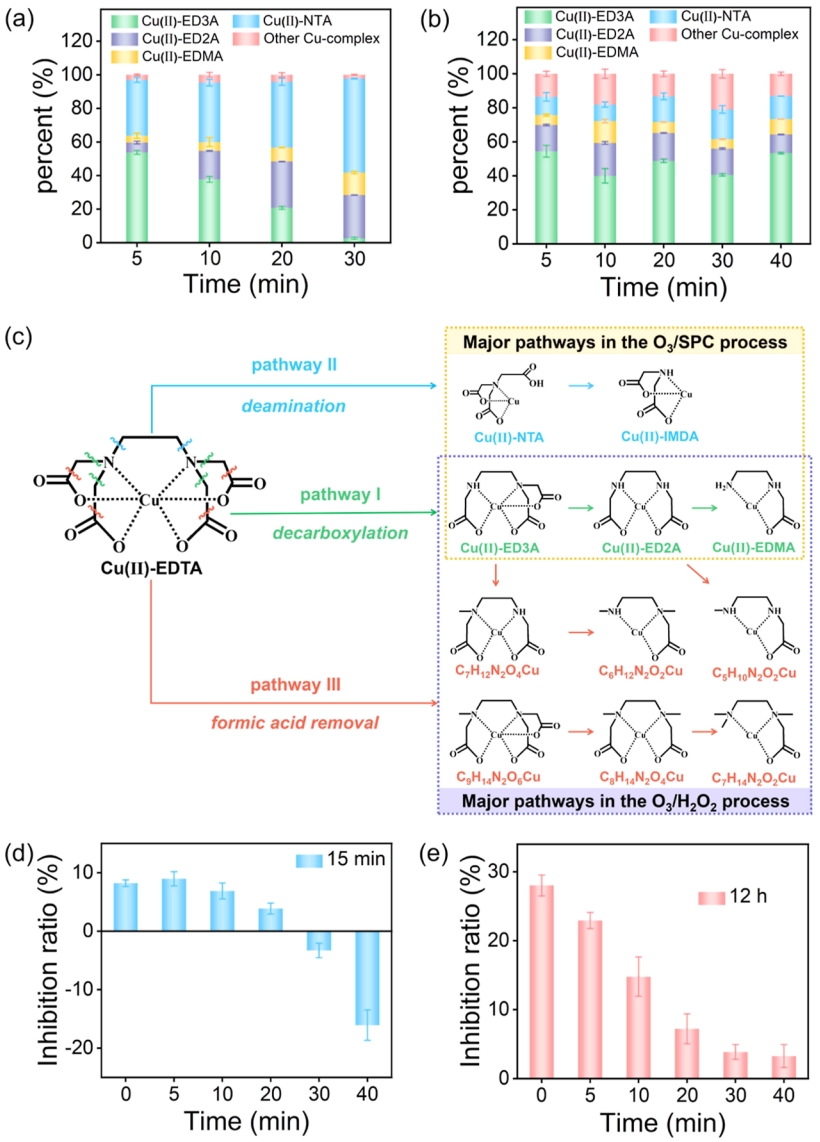

Figure 3. Proportions of Cu-containing intermediates as a function of reaction time in the processes of (a) O_3/SPC and (b) O_3/H_2O_2. (c) Major decomplexation pathways of Cu(II)−EDTA in the processes of O_3/SPC and O_3/H_2O_2. The substances inside the green, blue, and red frames represent the Cu-containing intermediates generated from pathways I, II, and III, respectively. Change in (d) acute and (e) chronic toxicities during Cu(II)−EDTA degradation in the O_3/SPC process. Experimental conditions: $[Cu(II)-EDTA]_0$ = 0.1 mM, $[O_3]$ = 0.3 mM, $[SPC]_0$ = 2 mM, $[H_2O_2]_0$ = 3 mM, and initial pH = 7.

$$Cu(II) + H_2O_2 \rightarrow Cu(I) + HO_2^{\bullet} + H^+ \quad k = 460 \pm 9\ M^{-1}\ s^{-1} \tag{14}$$

Decomplexation Pathways of Cu(II)−EDTA and Toxicity Assessment. It is acknowledged that $CO_3^{\bullet-}$ and $^{\bullet}OH$ as electrophilic radicals are inclined to attack the sites with high electrophilic values (f^-).[44,45] The ESP mapping result and the electron density isosurface of Fukui function f^- demonstrate that the amino group and the carboxyl group have higher potentials to be electrophilically attacked than the other groups in the Cu(II)−EDTA molecule (Figure 2a−c).[46] The calculation of the condensed Fukui function f^- further verifies that the amino group and carboxyl group are the electron-rich centers, and N3 (f^- = 0.035981), N4 (f^- = 0.036141), and all carboxyl oxygen are the susceptible sites for electrophilic attack (Table S2). However, the saturated bonds and high steric hindrance cause the high stability of carboxyl oxygen, implying that the carboxyl oxygen of Cu(II)−EDTA is improbable to be theoretically attacked.[47,48] Previous studies have reported that electrophilic radical is liable to break the C−C bond in C−COOH of the organic compound through a single-electron transfer pathway.[49,50] Thus, N3, N4, and C−C bonds of Cu(II)−EDTA are the most reactive sites for electrophilic radical attacking. Three possible decomplexation pathways of Cu(II)−EDTA are proposed (Figure 2d). In pathway I of decarboxylation, the cleavage of $N-CH_2$ bond in the $[-N-(CH_2-COOH)]$ group occurs with the removal of acetic acid, resulting in the formation of Cu(II)−ethylenediaminetriacetic acid (ED3A). Cu(II)−ethylenediamine-*N*,*N*′-diacetic acid (ED2A) and Cu(II)−ethylenediamineacetic acid (EDMA) can be generated through the continuous decarboxylation process.[1−4] In pathway II of deamination, the CH_2-N bond in the $[CH_2-N-(CH_2-COOH)_2]$ group of Cu(II)−EDTA is cleaved with the removal of iminodiacetic acid (IMDA) and then rapidly oxidized to generate Cu(II)−nitrilotriacetate acid

https://doi.org/10.1021/acs.est.3c00190
Environ. Sci. Technol. 2023, 57, 5034−5045

(NTA).[7−10] Pathways I and II have been previously reported in the decomplexation of Cu(II)−EDTA. In pathway III of formic acid removal, the C−C bond is cleaved in the [C−COOH] group with formic acid broken off. This pathway has not been considered in the relevant studies and will be discussed in detail.

The characteristics of $CO_3^{\bullet-}$ and $^{\bullet}OH$ are depicted in Figure 2e. Except for the fact that $CO_3^{\bullet-}$ has a much longer half-time than $^{\bullet}OH$, $CO_3^{\bullet-}$ can be considered a stronger electrophile than $^{\bullet}OH$ in terms of the lowest unoccupied molecular orbital (LUMO) and the electrophilic index.[18,51−53] To deeply investigate the difference in Cu(II)−EDTA decomplexation by $CO_3^{\bullet-}$/$^{\bullet}OH$ attack, the Gibbs free energies (ΔG) of the reaction between active species ($CO_3^{\bullet-}$ or $^{\bullet}OH$) and Cu(II)−EDTA in the three pathways are evaluated (Tables S3 and S4). As shown in Figure 2f,g, the reaction between active species ($CO_3^{\bullet-}$ or $^{\bullet}OH$) and Cu(II)−EDTA in each pathway is thermodynamically spontaneous. The calculated energy barriers are 23.2, 26.0, and 38.9 kcal mol^{-1} for decarboxylation, deamination, and removal of formic acid from Cu(II)−EDTA mediated by $CO_3^{\bullet-}$, respectively. In comparison, the energy barriers corresponding to decarboxylation, deamination, and formic acid removal from Cu(II)−EDTA mediated by $^{\bullet}OH$ are 26.5, 30.3, and 32.6 kcal mol^{-1}, respectively. These results determine that $CO_3^{\bullet-}$ is more active than $^{\bullet}OH$ to promote decarboxylation and deamination processes due to the lower energy barriers. Moreover, in the $CO_3^{\bullet-}$-mediated reactions, the energy barrier of formic acid removal from Cu(II)−EDTA is apparently higher than that of decarboxylation and deamination processes, testifying the regioselectivity of the $CO_3^{\bullet-}$ attack. Noticeably, the energy barrier difference between pathways II and III mediated by $^{\bullet}OH$ (2.3 kcal mol^{-1}) is significantly lower than that between the two pathways mediated by $CO_3^{\bullet-}$ (12.9 kcal mol^{-1}), implying that $^{\bullet}OH$ is more favorable to promote formic acid removal from Cu(II)−EDTA than $CO_3^{\bullet-}$. Thus, $^{\bullet}OH$ undergoes less selective reactions than $CO_3^{\bullet-}$ toward Cu(II)−EDTA.

To validate the above discussion, the Cu-containing intermediates in the O_3/SPC process were analyzed based on the LC−MS/MS analysis. As shown in Figure S12, the extracted ion chromatograms (EIC) and electrospray ionization-mass spectrometry (ESI-MS) of these decarboxylated [including Cu(II)−ED3A ([$C_8H_{12}N_2O_6Cu$ + H^+], m/z = 296.0072), Cu(II)−ED2A ([$C_6H_{10}N_2O_4Cu$ + H^+], m/z = 238.0008), Cu(II)−EDMA ([$C_4H_8N_2O_2Cu$ + H^+], m/z = 179.9959)] and deaminated intermediates [Cu(II)−NTA ([$C_6H_7NO_6Cu$−H^+], m/z = 250.9505)] were detected in the O_3/SPC process. According to the further EIS tandem mass spectrometry (ESI-MS^2) results, the detected ion clusters verified the existence of these decarboxylated and deaminated intermediates of Cu(II)−EDTA (Figure S13). It was obvious that the peak areas of the EIC and the ESI-MS spectra with relative intensities of these intermediates varied constantly with the reaction time. Additionally, the decomposition product of Cu(II)−NTA {Cu(II)−IMDA ([$C_4H_5NO_4Cu$ + H^+], m/z = 194.9592)} and the accumulation of generated iminodiacetic acid ([$C_4H_7NO_4$−H^+], m/z = 132.0302) were also observed during Cu(II)−EDTA degradation in the O_3/SPC process (Figures S14 and S15). These observations confirmed that $CO_3^{\bullet-}$-mediated decomplexation of Cu(II)−EDTA involved the continuous decarboxylation and deamination process. To assess the contribution of decarboxylation and deamination processes to Cu(II)−EDTA decomplexation, the molar concentrations of Cu(II)−EDTA and its Cu-containing intermediates were monitored in the O_3/SPC process. The concentrations of Cu(II)−ED3A, Cu(II)−ED2A, Cu(II)−EDMA, and Cu(II)−NTA quickly increased within the initial reaction time of 10 min and then decreased with time (Figure S16). The fractions of the four intermediates in the whole Cu-containing intermediates as functions of time were further calculated. As displayed in Figure 3a, the decarboxylated intermediates of Cu(II)−EDTA corresponded to the proportion of 41.8−63.7%, and the generated deaminated intermediate accounted for 33.2−56.0% during the reaction process. The proportion of decarboxylated and deaminated intermediates of Cu(II)−EDTA remained over 95.4%, which was in accordance with the aforementioned DFT results. The above results manifest that $CO_3^{\bullet-}$ selectively attacks the amino groups of Cu(II)−EDTA for the decarboxylation and deamination processes, resulting in the efficient conversion of decomplexed Cu into free Cu(II).

The EIC and ESI-MS spectra of the decarboxylated and deaminated intermediates of Cu(II)−EDTA detected in the O_3/H_2O_2 process are shown in Figure S17. The peak areas of the EIC and ESI-MS spectra with relative intensities of these intermediates in the O_3/H_2O_2 process were quite different from those in the O_3/SPC process. Considering that the O_3/H_2O_2 process presented a different Cu(II)−EDTA decomplexation trend, we further monitored the concentrations of Cu(II)−EDTA and its decarboxylated and deaminated intermediates during the reaction (Figure S18). Noticeably, the efficiency of Cu(II)−EDTA degradation in the O_3/H_2O_2 process (92.8%, 0.060 min^{-1}) was lower than that in the O_3/SPC process (100%, 0.138 min^{-1}) (Figure S19), which was in good agreement with the lower reactivity of $^{\bullet}OH$ with Cu(II)−EDTA. Moreover, the proportion of the decarboxylated intermediates (61.6−75.5%) was obviously higher than that of the deaminated intermediates (9.7−17.5%) during the decomplexation of Cu(II)−EDTA (Figure 3b). The result was ascribed to the lower energy barrier corresponding to decarboxylation mediated by $^{\bullet}OH$ (26.5 kcal mol^{-1}) compared with deamination (30.3 kcal mol^{-1}) from Cu(II)−EDTA. The other Cu-containing intermediates were identified by ESI-MS analysis, including P1 ($C_9H_{14}N_2O_6Cu$, m/z = 310.0221, +ESI), P2 ($C_8H_{14}N_2O_4Cu$, m/z = 266.0322, +ESI), P3 ($C_7H_{14}N_2O_2Cu$, m/z = 220.0279, −ESI), P4 ($C_7H_{12}N_2O_4Cu$, m/z = 252.0166, +ESI), P5 ($C_6H_{12}N_2O_2Cu$, m/z = 208.0269, +ESI), and P6 ($C_5H_{10}N_2O_2Cu$, m/z = 194.0111, +ESI) (Figure S20). The structures of P1−P6 were further evidenced by their ESI-MS^2 spectra, indicating that they were the products corresponding to the formic acid removal from Cu(II)−EDTA and its decarboxylated intermediates. This degradation pathway confirms that the C−C bond in C−COOH group of Cu(II)−EDTA is the susceptible site for $^{\bullet}OH$ attack.

Figure 3c further presented and compared the major decomplexation pathways of Cu(II)−EDTA in the processes of O_3/SPC and O_3/H_2O_2. It was apparent that the O_3/SPC process could achieve efficient decarboxylation and deamination processes by $CO_3^{\bullet-}$ attack, facilitating the successive cleavage of Cu−O and Cu−N bonds in the Cu(II)−EDTA complex. In comparison, O_3/H_2O_2 mainly induced the breakage of Cu−O bonds via decarboxylation and formic acid removal, which substantially impeded the release of Cu(II) from the Cu(II)−EDTA complex. Moreover, the low

https://doi.org/10.1021/acs.est.3c00190
Environ. Sci. Technol. 2023, 57, 5034−5045

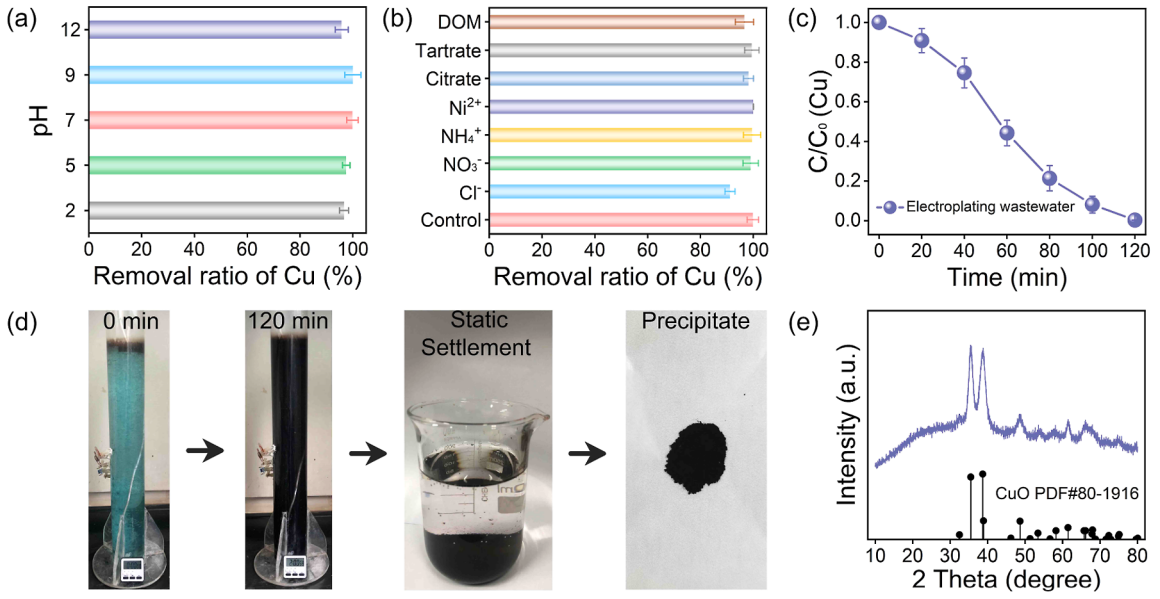

Figure 4. Effect of pH (a) and coexisting substances (b) on Cu recovery in the O_3/SPC process. Changes of Cu recovery (c) and solution color (d) in the treatment of real copper electroplating wastewater by O_3/SPC. (e) XRD pattern of the obtained precipitate in the treatment of real copper electroplating wastewater by O_3/SPC. Experimental conditions: $[Cu(II)-EDTA]_0$ = 0.1 mM, $[O_3]$ = 0.3 mM, $[SPC]_0$ = 2 mM, [inorganic ions] = 0.5 mM, [citrate or tartrate] = 0.1 mM, and [DOM] = 20 mg_C L^{-1}.

degradation rate of Cu(II)−EDTA and a high level of TOC removal efficiency in the O_3/H_2O_2 process illustrated that $^{\bullet}OH$ tended to react with small-molecule substances from Cu(II)−EDTA decomplexation, resulting in the low utilization efficiency of $^{\bullet}OH$ for the targeted attack of Cu(II)−EDTA. These observations well explained why the low decomplexation rate of Cu(II)−EDTA was usually observed in $^{\bullet}OH$-based oxidation processes. It can be concluded that the $CO_3^{\bullet-}$-mediated O_3/SPC process outperforms traditional oxidation processes for the targeted decomplexation of Cu(II)−EDTA, thus accelerating Cu recovery efficiency.

The acute and chronic toxicities of the degradation intermediates and products of Cu(II)−EDTA in the O_3/SPC process were assessed using the *Vibrio qinghaiensis* sp.-*Q67* luminescence inhibition test.[7] As shown in Figure 3d, the inhibition ratio of the untreated Cu(II)−EDTA solution was approximately 8% in the acute toxicity test, while the inhibition ratio slightly increased to the maximum value in the first 5 min. The inhibition ratio distinctly decreased as the reaction proceeded, and even the promoting effect was observed after 30 min. The results indicated that no acute toxicity products were obtained after O_3/SPC treatment. In the chronic toxicity test, compared with the 28.0% luminescence inhibition effect caused by the initial Cu(II)−EDTA solution, the gradually decreasing luminescence inhibition effects of the Cu(II)−EDTA solution samples were recorded in the O_3/SPC process (Figure 3e). The final products of Cu(II)−EDTA showed nearly no chronic toxicity in *Vibrio qinghaiensis* sp.-*Q67* due to the less than 3.5% luminescence inhibition ratio. These results clearly suggest that the O_3/SPC process is superior to other reported processes with respect to environmental decontamination, resulting from the generation of toxic-free byproducts.

Applicability Analysis of the O_3/SPC Process. We investigated the effects of typical influence factors (such as solution pH and coexisting substances) on the Cu recovery performance in the O_3/SPC process. As shown in Figure 4a, the O_3/SPC process exhibited excellent Cu recovery efficiency (95.7−100%) from the Cu(II)−EDTA complex under broad initial pH range conditions (2.0−12.0), which was better than the previously mentioned processes, such as the electro-Fenton process, discharge plasma oxidation, and UV/persulfate.[2,8,12] The phenomenon was ascribed to the fact that SPC could maintain the alkalinity of the reaction solution regardless of the initial pH value (Figure S21).[54] We further investigated the recovery performance of Cu in the O_3/SPC process by preintroducing SPC before adjusting the solution pH (7.0−11.0) (Figure S22). The experimental results revealed that efficient performance of the O_3/SPC process for Cu recovery could be achieved except for the pH of 7.0. The observation was due to a few $CO_3^{\bullet-}$ initiated by the peroxone reaction and the process between $^{\bullet}OH$ and HCO_3^- ($k = 8.5 \times 10^6$ M^{-1} s^{-1}) in the O_3/SPC process at a pH of 7.0.[12,35] Besides, the influence of typical inorganic ions (such as Cl^-, NO_3^-, NH_4^+, and Ni^{2+}) and organic molecules [such as citrate, tartrate, and dissolved organic matter (DOM)] on the O_3/SPC process was investigated. As observed in Figure 4b, after the addition of NO_3^- and NH_4^+, there was no distinct influence on the recovery of Cu. The coexisting Ni^+ might consume active species and carbonate in the O_3/SPC process, affecting Cu recovery. However, the effect of Ni^{2+} on Cu recovery was negligible due to the complexing competitive effect of Ni^+ with EDTA and the compensation effect of the formation of $CO_3^{\bullet-}$ via the reaction of Ni^{2+}, H_2O_2, and carbonate.[9] In the presence of Cl^-, the recovery efficiency of Cu decreased to 91.2%. The decrease is attributed to the consumption of $^{\bullet}OH$ by Cl^- in the O_3/SPC process to form active chlorine species (Cl_2 and ClO^-), which barely react with Cu(II)−EDTA as previous studies reported (Figure S23).[14,55,56] Cl_2 (E^0 = 1.36 V vs SHE) and ClO^- (E^0 = 0.89 V vs SHE) have lower reduction potentials than $CO_3^{\bullet-}$ (E^0 = 1.78 V vs SHE), revealing that Cu(II)−EDTA is preferentially oxidized by $CO_3^{\bullet-}$ but not the active chlorine species.[57] As such, toxic organochlorines would not be generated in the reaction process. In addition, with the assistance of LC−MS/MS analysis, the chlorinated byproducts

https://doi.org/10.1021/acs.est.3c00190
Environ. Sci. Technol. 2023, 57, 5034−5045

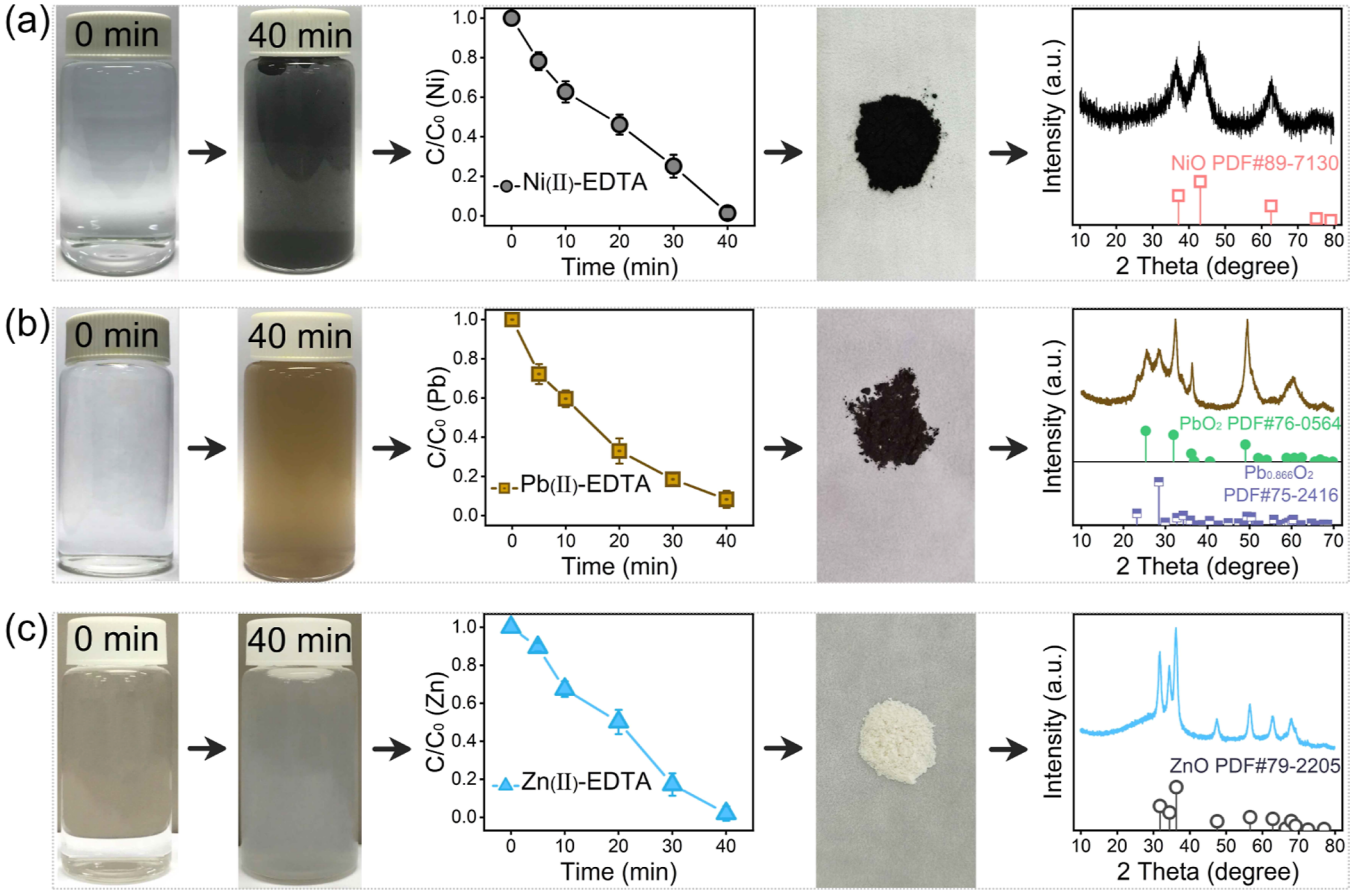

Figure 5. Changes of metal recovery and solution color in the treatment of metal−EDTA complexes in the O_3/SPC process [(a) Ni(II)−EDTA, (b) Pb(II)−EDTA, and (c) Zn(II)−EDTA] and the XRD patterns of the corresponding metal-precipitates. Experimental conditions: [metal−EDTA]$_0$ = 0.1 mM, [O_3] = 0.3 mM, [SPC]$_0$ = 2 mM, and initial pH = 7.

of Cu(II)−EDTA decomplexation and the chlorinated small molecules (such as dichloroacetic acid and trichloroacetic acid) were not detected in the treatment of Cl^--containing Cu(II)−EDTA wastewater by the O_3/SPC process. In the presence of citrate and tartrate, the recovery efficiencies of Cu reached 98.2 and 99.4%, respectively. The addition of DOM had a slight effect on Cu recovery in the O_3/SPC process. This was because $CO_3^{\bullet-}$ was more selective than $^{\bullet}OH$, and the reaction rates of $CO_3^{\bullet-}$ with DOM were 2 orders of magnitude slower than those of $^{\bullet}OH$ with DOM.[17,58] These results illustrate that the O_3/SPC process is a promising option for efficient Cu recovery from real wastewater.

To investigate the feasibility of employing the O_3/SPC process for the treatment of real copper electroplating industrial wastewater, technical optimization was performed since the treatment performance could be affected by plenty of coexisting substances (Table S1). As shown in Figure 4c, the optimized O_3/SPC process [including ozone concentration (0.4 mM), O_3 flow rate (800 mL min^{-1}), and SPC dosage (20 mM)] could provide an endogenous alkaline condition during the reaction process and decrease the concentration of Cu from 228 mg L^{-1} to the value (0.29 mg L^{-1}) below the electroplating discharge limit (GB21900-2008, China) within 120 min. Moreover, the distinct color change of the reaction solution (from blue to dark) confirmed that the O_3/SPC process could attack the complexed Cu(II) in real wastewater (Figure 4d). After the treatment, the dark precipitate was finally collected after static settlement, which was identified as CuO by the XRD pattern (Figure 4e). The phenomenon was consistent with the above-mentioned experiment of Cu(II)−EDTA degradation in the O_3/SPC process. Furthermore, the corresponding electrical energy per order (EEO) value of the O_3/SPC process in the treatment of real copper electroplating wastewater was estimated to be 0.108 kW h g^{-1} with reference to the recovery of Cu, which was much less than that in other oxidation processes, such as UV/chlorine (7.740 kW h g^{-1}) and electrolysis-O_3 with the Ti cathode (634.461 kW h g^{-1}) (Table S5).[14,59] The above performance results validate the superior ability of the O_3/SPC process reported in this work for both metal resource recovery from heavy metal complex wastewater and environmental decontamination compared with the common treatment processes.

The applicability of the O_3/SPC process with respect to the EDTA-complexed Ni(II), Pb(II), and Zn(II) was further performed. As presented in Figure 5a, the color of Ni(II)−EDTA solution distinctly changed to black from light blue in the O_3/SPC process, and the aqueous concentration of Ni was reduced to 0.08 mg L^{-1} from 5.87 mg L^{-1} within 40 min. The XRD pattern of the obtained black precipitate was associated with NiO (JCPDS no. 89-7130). These results indicate that the O_3/SPC process exhibits superior Ni recovery capacity in treating the Ni(II)−EDTA complex, resulting in the generation of NiO. In addition, the change of Pb(II)−EDTA solution color (from colorless to brown) also implied that the decomplexed Pb could be efficiently recovered in the O_3/SPC process. As illustrated in Figure 5b, about 92% of aqueous Pb

https://doi.org/10.1021/acs.est.3c00190
Environ. Sci. Technol. 2023, 57, 5034−5045

was transformed to Pb precipitate within 40 min. The XRD pattern of the brown precipitate corresponded to PbO_2 (JCPDS no. 76-0564) and $Pb_{0.866}O_2$ (JCPDS no. 75-2416). As for Zn(II)−EDTA, the solution in the O_3/SPC process changed to white from colorless (Figure 5c). The O_3/SPC process recovered 98.0% of the decomplexed Zn, and the aqueous concentration of Zn was less than 0.14 mg L^{-1} after 40 min. The white precipitate was identified as ZnO by XRD analysis (JCPDS no. 79-2205). Considering the coexistence phenomenon of metal complexes in real industrial wastewater, the metal recovery efficiency of the blended system was further explored by the O_3/SPC process. As shown in Figure S25, the O_3/SPC process could achieve 100% metal recovery in the blended Cu(II)/Ni(II)−EDTA systems. These results demonstrate that the O_3/SPC process has good application potential to recover metal resources of metal complexes, leading to the formation of stable metallic oxide.

■ ENVIRONMENTAL IMPLICATIONS

Metal−organic complexes are the common organics in industrial wastewater at high concentrations. Besides, the annual discharge of wastewater containing metal−organic complexes reaches up to million tons. Hence, recovering metal resources from metal−organic complex wastewater is of great interest under the background of sustainable development. Note that the breakage of metal−organic bonds is crucial for the recovery of metal from metal−organic complexes. In this study, the O_3/SPC process employing the generated $CO_3^{\bullet-}$ as a selective radical is proposed to accurately attack the electron-rich amino groups of Cu(II)−EDTA for efficient breakage of the metal−organic bonds (i.e., Cu−O and Cu−N bonds), achieving 100% Cu recovery. By comparison, the typical $^{\bullet}OH$-based O_3/H_2O_2 process mainly breaks Cu−O bonds via decarboxylation and formic acid removal, leading to inefficient Cu recovery. The price of industrial grade SPC (theoretically for $Na_2CO_3{\cdot}1.5H_2O_2$ calc. 32.5% H_2O_2), liquid H_2O_2 (i.e., 30% H_2O_2), and Na_2CO_3 are about 550, 500, and 20 $/metric ton, respectively (data from http://www.alibaba.com/).[60,61] Thereby, the cost of the combination of liquid H_2O_2 and Na_2CO_3 is 520 $/metric ton, which is slightly lower than that of SPC (550 $/metric ton). However, SPC does not have the extra cost in the terms of special facilities and practitioners for transportation and storage, which can compensate for its little higher chemical cost than liquid H_2O_2. Thus, SPC is widely acknowledged to be cheaper and more convenient than the combination of liquid H_2O_2 and Na_2CO_3 for practical application. Besides, the O_3/SPC process does not require extra alkali addition, which is dependent on the existing CO_3^{2-} to transform free Cu(II) into the stable Cu precipitate. It is evident that the O_3/SPC process has high applicability to recover Cu from real copper electroplating wastewater with low electrical energy consumption (0.108 kW h g^{-1}). This result also shows that the cost of the O_3/SPC process for scale-up implementation can be acceptable. In addition, toxic-free byproducts produced from the O_3/SPC process meets the biotoxicity requirement of the subsequent biological posttreatment, facilitating the sustainability of the metal−EDTA complex wastewater treatment. The O_3/SPC process also shows good application potential in treating other metal−organic complexes. This work reveals the decomplexation mechanisms of metal−organic complexes and highlights the good application potential of using the O_3/SPC process to achieve the efficient breakage of metal−organic bonds with simultaneous metal recovery from metal−organic complexes wastewater.

■ ASSOCIATED CONTENT

Supporting Information

The Supporting Information is available free of charge at https://pubs.acs.org/doi/10.1021/acs.est.3c00190.

Chemicals and reagents; performance evaluation of Cu recovery; determination of TOC removal; characterization methods of the precipitate; experimental details on EPR trapping measurement; identification of the inhibitory effect of active species scavenger; analytical methods of Cu(II)−EDTA and its intermediates; DFT calculation methods; electrical energy consumption calculation method; results on Cu recovery and TOC removal analysis; XRD patterns and XPS spectra of the precipitate; determination of radicals and radical quenching results; comparison on Cu-containing intermediates in the processes of O_3/SPC and O_3/H_2O_2, including mass spectra and quantification analysis; toxicity assessment of degradation intermediates and products; pH effect on Cu recovery; water quality parameters of real copper electroplating wastewater; calculated condensed Fukui function f^- of different atoms in the Cu(II)−EDTA molecule; states of the reaction between radicals and Cu(II)−EDTA in different pathways; and comparison of Cu recovery energy consumption of the O_3/SPC process and other reported processes (PDF)

■ AUTHOR INFORMATION

Corresponding Author

Jian-Ping Zou − *Key Laboratory of Jiangxi Province for Persistent Pollutants Control and Resources Recycle, Nanchang Hangkong University, Nanchang 330063, P. R. China;* orcid.org/0000-0002-3585-6541; Email: zjp_112@126.com

Authors

Ying Chen − *Key Laboratory of Jiangxi Province for Persistent Pollutants Control and Resources Recycle, Nanchang Hangkong University, Nanchang 330063, P. R. China; Key Laboratory of Poyang Lake Environment and Resource Utilization, Ministry of Education, School of Resources & Environment, Nanchang University, Nanchang 330031, P. R. China*

Yi Mu − *Key Laboratory of Jiangxi Province for Persistent Pollutants Control and Resources Recycle, Nanchang Hangkong University, Nanchang 330063, P. R. China;* orcid.org/0000-0001-9176-5049

Lei Tian − *Key Laboratory of Jiangxi Province for Persistent Pollutants Control and Resources Recycle, Nanchang Hangkong University, Nanchang 330063, P. R. China*

Ling-Ling Zheng − *Key Laboratory of Jiangxi Province for Persistent Pollutants Control and Resources Recycle, Nanchang Hangkong University, Nanchang 330063, P. R. China*

Yi Mei − *Key Laboratory of Jiangxi Province for Persistent Pollutants Control and Resources Recycle, Nanchang Hangkong University, Nanchang 330063, P. R. China*

Qiu-Ju Xing − *Key Laboratory of Jiangxi Province for Persistent Pollutants Control and Resources Recycle,*

https://doi.org/10.1021/acs.est.3c00190
Environ. Sci. Technol. 2023, 57, 5034−5045

Nanchang Hangkong University, Nanchang 330063, P. R. China

Wen Liu − *The Key Laboratory of Water and Sediment Sciences (Ministry of Education), College of Environmental Sciences and Engineering, Peking University, Beijing 100871, P. R. China;* orcid.org/0000-0002-6787-2431

Lixia Yang − *Key Laboratory of Jiangxi Province for Persistent Pollutants Control and Resources Recycle, Nanchang Hangkong University, Nanchang 330063, P. R. China;* orcid.org/0000-0002-0982-9881

Shenglian Luo − *Key Laboratory of Jiangxi Province for Persistent Pollutants Control and Resources Recycle, Nanchang Hangkong University, Nanchang 330063, P. R. China;* orcid.org/0000-0002-0802-1629

Daishe Wu − *Key Laboratory of Poyang Lake Environment and Resource Utilization, Ministry of Education, School of Resources & Environment, Nanchang University, Nanchang 330031, P. R. China; School of Materials and Chemical Engineering, Pingxiang University, Pingxiang 337000, P. R. China*

Complete contact information is available at: https://pubs.acs.org/10.1021/acs.est.3c00190

Author Contributions

[⊥]Y.C. and Y.M. contributed equally to this work.

Notes

The authors declare no competing financial interest.

■ ACKNOWLEDGMENTS

This work was supported by the National Science Foundation of China (52170082, 51868050, 51878325, 51938007, and 21906076), and the Natural Science Foundation of Jiangxi Province (20212ACB203008).

■ REFERENCES

(1) Xu, Z.; Zhang, Q. R.; Li, X. C.; Huang, X. F. A critical review on chemical analysis of heavy metal complexes in water/wastewater and the mechanism of treatment methods. *Chem. Eng. J.* **2022**, *429*, 131688−131704.

(2) Li, M. Q.; Chen, N.; Shang, H.; Ling, C. C.; Wei, K.; Zhao, S. X.; Zhou, B.; Jia, F. L.; Ai, Z. H.; Zhang, L. Z. An electrochemical strategy for simultaneous heavy metal complexes wastewater treatment and resource recovery. *Environ. Sci. Technol.* **2022**, *56*, 10945−10953.

(3) Liu, Y.; Feng, Y.; Zhang, Y. F.; Mao, M.; Wu, D. L.; Chu, H. Q. Highly efficient degradation of dimethyl phthalate from Cu(II) and dimethyl phthalate wastewater by EDTA enhanced ozonation: Performance, intermediates and mechanism. *J. Hazard. Mater.* **2019**, *366*, 378−385.

(4) Lan, S. Y.; Xiong, Y.; Tian, S. H.; Feng, J. X.; Xie, T. Y. Enhanced self-catalytic degradation of CuEDTA in the presence of H_2O_2/UV: Evidence and importance of Cu-peroxide as a photo-active intermediate. *Appl. Catal., B* **2016**, *183*, 371−376.

(5) Li, J. Y.; Ma, J. X.; Dai, R. B.; Wang, X. Y.; Chen, M.; Waite, T.; Wang, Z. W. Self-enhanced decomplexation of Cu-Organic complexes and Cu recovery from wastewaters using an electrochemical membrane filtration system. *Environ. Sci. Technol.* **2021**, *55*, 655−664.

(6) Yuan, Y.; Zhao, W.; Liu, Z. C.; Ling, C.; Zhu, C. Q.; Liu, F. Q.; Li, A. M. Low-Fe(III) driven UV/Air process for enhanced recovery of heavy metals from EDTA complexed system. *Water Res.* **2020**, *171*, 115375−115386.

(7) Zhang, L.; Wu, B. D.; Zhang, G. Y.; Gan, Y. H.; Zhang, S. J. Enhanced decomplexation of Cu(II)-EDTA: The role of acetylacetone in Cu-mediated photo-Fenton reactions. *Chem. Eng. J.* **2019**, *358*, 1218−1226.

(8) Wang, T. C.; Cao, Y.; Qu, G. Z.; Sun, Q. H.; Xia, T. J.; Guo, X. T.; Jia, H. Z.; Zhu, L. Y. Novel Cu(II)−EDTA decomplexation by discharge plasma oxidation and coupled Cu removal by alkaline precipitation: Underneath mechanisms. *Environ. Sci. Technol.* **2018**, *52*, 7884−7891.

(9) Cao, Y.; Qian, X. C.; Zhang, Y. X.; Qu, G. Z.; Xia, T. J.; Guo, X. T.; Jia, H. Z.; Wang, T. C. Decomplexation of EDTA-chelated copper and removal of copper ions by non-thermal plasma oxidation/alkaline precipitation. *Chem. Eng. J.* **2019**, *362*, 487−496.

(10) Hu, X. X.; Yang, S.; You, X. Y.; Zhang, W. W.; Liu, Y.; Liang, W. Y. Electrocatalytic decomplexation of Cu-EDTA and simultaneous recovery of Cu with Ni/GO-PAC particle electrode. *Chem. Eng. J.* **2022**, *428*, 131468−131481.

(11) Guan, Z. J.; Guo, Y. P.; Huang, Z. H.; Liao, X. J.; Chen, S. J.; Ou, X. L.; Sun, S. Y.; Liang, J. L.; Cai, Y. F.; Xie, W. R.; Xian, J. Simultaneous and efficient removal of organic Ni and Cu complexes from electroless plating effluent using integrated catalytic ozonation and chelating precipitation process in a continuous pilot-scale system. *Chem. Eng. J.* **2022**, *428*, 131250−131262.

(12) Xu, Z.; Shan, C.; Xie, B. H.; Liu, Y.; Pan, B. C. Decomplexation of Cu(II)-EDTA by UV/persulfate and UV/H_2O_2: Efficiency and mechanism. *Appl. Catal., B* **2017**, *200*, 439−447.

(13) Zhang, Y.; Sun, J.; Guo, Z. W.; Zheng, X. Q.; Guo, P. R.; Xu, J. W.; Lei, Y. Q. The decomplexation of Cu-EDTA by electro-assisted heterogeneous activation of persulfate via acceleration of Fe(II)/Fe(III) redox cycle on Fe-MOF catalyst. *Chem. Eng. J.* **2022**, *430*, 133025−133034.

(14) Huang, X. F.; Wang, Y.; Li, X. C.; Guan, D. X.; Li, Y. B.; Zheng, X. Y.; Zhao, M.; Shan, C.; Pan, B. C. Autocatalytic Decomplexation of Cu(II)−EDTA and simultaneous removal of aqueous Cu(II) by UV/Chlorine. *Environ. Sci. Technol.* **2019**, *53*, 2036−2044.

(15) Xu, H. L.; Chen, R. D.; Liang, S.; Lei, Z. C.; Zheng, W. X.; Yan, Z.; Cao, J. X.; Wei, C. H.; Feng, C. H. Minimizing toxic chlorinated byproducts during electrochemical oxidation of Ni-EDTA: Importance of active chlorine-triggered Fe(II) transition to Fe(IV). *Water Res.* **2022**, *219*, 118548−118557.

(16) Feng, H. L.; Liao, X. Q.; Yang, R. L.; Chen, S. H.; Zhang, Z. J.; Tong, J. S.; Liu, J. J.; Wang, X. J. Generation, toxicity, and reduction of chlorinated byproducts: Overcome bottlenecks of electrochemical advanced oxidation technology to treat high chloride wastewater. *Water Res.* **2023**, *230*, 119531−119541.

(17) Wojnárovits, L.; Tóth, T.; Takács, E. Rate constants of carbonate radical anion reactions with molecules of environmental interest in aqueous solution: A review. *Sci. Total Environ.* **2020**, *717*, 137219−137242.

(18) Min, S. J.; Kim, J. G.; Baek, K. Role of carbon fiber electrodes and carbonate electrolytes in electrochemical phenol oxidation. *J. Hazard. Mater.* **2020**, *400*, 123083−123090.

(19) Alegre, M. L.; Geronés, M.; Rosso, J. A.; Bertolotti, S. G.; Braun, A. M.; Mártire, D. O.; Gonzalez, M. C. Kinetic study of the reactions of chlorine atoms and $Cl_2^{\bullet-}$ radical anions in aqueous solutions. 1. reaction with benzene. *J. Phys. Chem. A* **2000**, *104*, 3117−3125.

(20) Chen, F. Y.; Xia, L. G.; Zhang, Y.; Bai, J.; Wang, J. C.; Li, J. H.; Rahim, M.; Xu, Q. J.; Zhu, X. Y.; Zhou, B. X. Efficient degradation of refractory organics for carbonate-containing wastewater via generation carbonate radical based on a photoelectrocatalytic TNA-MCF system. *Appl. Catal., B* **2019**, *259*, 118071−118077.

(21) Kong, X. J.; Wang, L. P.; Wu, Z. H.; Zeng, F. L.; Sun, H. Y.; Guo, K. H.; Hua, Z. C.; Fang, J. Y. Solar irradiation combined with chlorine can detoxify herbicides. *Water Res.* **2020**, *177*, 115784−115794.

(22) Hao, Z. Y.; Ma, J. Z.; Miao, C. Y.; Song, Y.; Lian, L. S.; Yan, S. W.; Song, W. H. Carbonate radical oxidation of cylindrospermopsin (cyanotoxin): Kinetic studies and mechanistic consideration. *Environ. Sci. Technol.* **2020**, *54*, 10118−10127.

(23) Chen, Z. F.; Meyer, T. J. Copper(II) catalysis of water oxidation. *Angew. Chem., Int. Ed.* **2013**, *52*, 700−703.

(24) Xue, B. W.; Qv, C.; Qian, Z. W.; Han, C. Y.; Luo, G. X. Synthesis of CuO from $CuCO_3{\cdot}Cu(OH)_2$ and its catalytic activity in the degradation of methylene blue. *Res. Chem. Intermed.* **2017**, *43*, 911−926.
(25) Wang, T. C.; Wang, Q.; Soklun, H.; Qu, G. H.; Xia, T. J.; Guo, X. T.; Jia, H. Z.; Zhu, L. Y. A green strategy for simultaneous Cu(II)-EDTA decomplexation and Cu precipitation from water by bicarbonate-activated hydrogen peroxide/chemical precipitation. *Chem. Eng. J.* **2019**, *370*, 1298−1309.
(26) He, J.; Song, W. C.; Huang, X. H.; Gao, Z. Y. Preparation, characterization, and catalytic activity of a novel MgO/expanded graphite for ozonation of Cu-EDTA. *Environ. Sci. Pollut. Res.* **2021**, *28*, 39513−39523.
(27) Yu, X. B.; Kamali, M.; Van Aken, P. V.; Appels, L.; Van der Bruggen, B. V.; Dewil, R. Synergistic effects of the combined use of ozone and sodium percarbonate for the oxidative degradation of dichlorvos. *J. Water Proc. Eng.* **2021**, *39*, 101721−101728.
(28) Guo, H.; Li, D. S.; Li, Z.; Lin, S. Y.; Wang, Y. W.; Pan, S. J.; Han, J. G. Promoted elimination of antibiotic sulfamethoxazole in water using sodium percarbonate activated by ozone: Mechanism, degradation pathway and toxicity assessment. *Sep. Purif. Technol.* **2021**, *266*, 118543−118554.
(29) Gao, J.; Duan, X. D.; O'Shea, K.; Dionysiou, D. D. Degradation and transformation of bisphenol A in UV/Sodium percarbonate: Dual role of carbonate radical anion. *Water Res.* **2020**, *171*, 115394−115403.
(30) Gao, J.; Song, J.; Ye, J. S.; Duan, X. D.; Dionysiou, D. D.; Yadav, J. S.; Nadagouda, M. N.; Yang, L. X.; Luo, S. L. Comparative toxicity reduction potential of UV/sodium percarbonate and UV/hydrogen peroxide treatments for bisphenol A in water: An integrated analysis using chemical, computational, biological, and metabolomic approaches. *Water Res.* **2021**, *190*, 116755−116766.
(31) Song, Y. Q.; Zhao, C.; Wang, T.; Kong, Z.; Zheng, L. S.; Ding, H. J.; Liu, Y. Y.; Zheng, H. L. Simultaneously promoted reactive manganese species and hydroxyl radical generation by electro-permanganate with low additive ozone. *Water Res.* **2021**, *189*, 116623−116632.
(32) Li, Y. F.; Zhu, Y. Q.; Wang, D. B.; Yang, G. J.; Pan, L. Y.; Wang, Q. L.; Ni, B. J.; Li, H. L.; Yuan, X. Z.; Jiang, L. B.; Tang, W. W. Fe(II) catalyzing sodium percarbonate facilitates the dewaterability of waste activated sludge: Performance, mechanism, and implication. *Water Res.* **2020**, *174*, 115626−115638.
(33) Asghar, A.; Lutze, H. V.; Tuerk, J.; Schmidt, T. C. Influence of water matrix on the degradation of organic micropollutants by ozone based processes: A review on oxidant scavenging mechanism. *J. Hazard. Mater.* **2022**, *429*, 128189−128213.
(34) Huang, X. F.; Xu, Y.; Shan, C.; Li, X. C.; Zhang, W. M.; Pan, B. C. Coupled Cu(II)-EDTA degradation and Cu(II) removal from acidic wastewater by ozonation: Performance, products and pathways. *Appl. Catal., B* **2016**, *299*, 23−29.
(35) Guo, Z.; Xie, Y. B.; Xiao, J. D.; Zhao, Z.-J.; Wang, Y.; Xu, Z.; Zhang, Y.; Yin, L.; Cao, H.; Gong, J. Single-atom $Mn-N_4$ site-catalyzed peroxone reaction for the efficient production of hydroxyl radicals in an acidic solution. *J. Am. Chem. Soc.* **2019**, *141*, 12005−12010.
(36) Chen, H.; Wang, J. L. Degradation and mineralization of ofloxacin by ozonation and peroxone (O_3/H_2O_2) process. *Chemosphere* **2021**, *269*, 128775−128782.
(37) Zeng, H. B.; Liu, S. S.; Chai, B. Y.; Cao, D.; Wang, Y.; Zhao, X. Enhanced Photoelectrocatalytic Decomplexation of Cu−EDTA and Cu Recovery by Persulfate Activated by UV and Cathodic Reduction. *Environ. Sci. Technol.* **2016**, *50*, 6459−6466.
(38) Xu, H. Z.; Pang, Y. M.; Li, Y. Z.; Zhang, S. S.; Pei, H. Y. Using sodium percarbonate to suppress vertically distributed filamentous cyanobacteria while maintaining the stability of microeukaryotic communities in drinking water reservoirs. *Water Res.* **2021**, *197*, 117111−117121.
(39) Zhu, M.; Zhang, L. S.; Liu, S. S.; Wang, D. K.; Qin, Y. C.; Chen, Y.; Dai, W. L.; Wang, Y. H.; Xing, Q. J.; Zou, J. P. Degradation of 4-nitrophenol by electrocatalysis and advanced oxidation processes using Co_3O_4@C anode coupled with simultaneous CO_2 reduction via SnO_2/CC cathode. *Chin. Chem. Lett.* **2020**, *31*, 1961−1965.
(40) Gu, Z. N.; Zhang, Z. Y.; Ni, N.; Hu, C. Z.; Qu, J. H. Simultaneous Phenol Removal and Resource Recovery from Phenolic Wastewater by Electrocatalytic Hydrogenation. *Environ. Sci. Technol.* **2022**, *56*, 4356−4366.
(41) Khuntia, S.; Majumder, S. K.; Ghosh, P. Catalytic ozonation of dye in a microbubble system: Hydroxyl radical contribution and effect of salt. *J. Environ. Chem. Eng.* **2016**, *4*, 2250−2258.
(42) Sun, F. W.; Chen, T. H.; Chu, Z. Y.; Zhai, P. X.; Liu, H. B.; Wang, Q.; Zou, X. H.; Chen, D. The synergistic effect of calcite and Cu^{2+} on the degradation of sulfadiazine via PDS activation: A role of Cu(III). *Water Res.* **2022**, *219*, 118529−118538.
(43) Wang, L. H.; Xu, H. D.; Jiang, N.; Wang, Z. M.; Jiang, J.; Zhang, T. Trace cupric species triggered decomposition of peroxymonosulfate and degradation of organic pollutants: Cu(III) being the primary and selective intermediate oxidant. *Environ. Sci. Technol.* **2020**, *54*, 4686−4694.
(44) Liu, Y. Q.; He, X. X.; Duan, X. D.; Fu, Y. S.; Fatta-Kassinos, D.; Dionysiou, D. D. Significant role of UV and carbonate radical on the degradation of oxytetracycline in UV-AOPs: Kinetics and mechanism. *Water Res.* **2016**, *95*, 195−204.
(45) Li, H.; Sun, S. T.; Ji, H. D.; Liu, W.; Shen, Z. R. Enhanced activation of molecular oxygen and degradation of tetracycline over Cu-S_4 atomic clusters. *Appl. Catal., B* **2020**, *272*, 118966−118974.
(46) Liu, L. Q.; Deng, S. S.; Bao, Y. X.; Huang, J.; Yu, G. Degradation of OBS (sodium p-perfluorous nonenoxybenzenesulfonate) as a novel per- and polyfluoroalkyl substance by UV/persulfate and UV/sulfite: Fluorinated intermediates and treatability in fluoroprotein foam. *Environ. Sci. Technol.* **2022**, *56*, 6201−6211.
(47) Qi, J. J.; Yang, X. Y.; Pan, P. Y.; Huang, T. B.; Yang, X. D.; Wang, C. C.; Liu, W. Interface engineering of $Co(OH)_2$ nanosheets growing on the $KNbO_3$ perovskite based on electronic structure modulation for enhanced peroxymonosulfate activation. *Environ. Sci. Technol.* **2022**, *56*, 5200−5212.
(48) Li, N.; Li, R.; Duan, X. G.; Yan, B. B.; Liu, W.; Cheng, Z. J.; Chen, G. Y.; Hou, L.; Wang, S. B. Correlation of active sites to generated reactive species and degradation routes of organics in peroxymonosulfate activation by Co-loaded carbon. *Environ. Sci. Technol.* **2021**, *55*, 16163−16174.
(49) Zhou, Y. J.; Chen, C. Y.; Guo, K. H.; Wu, Z. H.; Wang, L. P.; Hua, Z. C.; Fang, J. Y. Kinetics and pathways of the degradation of PPCPs by carbonate radicals in advanced oxidation processes. *Water Res.* **2020**, *185*, 116231−116243.
(50) Dulova, N.; Kattel, E.; Trapido, M. Degradation of naproxen by ferrous ion-activated hydrogen peroxide, persulfate and combined hydrogen peroxide/persulfate processes: The effect of citric acid addition. *Chem. Eng. J.* **2017**, *318*, 254−263.
(51) Mittal, A.; Kakkar, R. The antioxidant potential of retrochalcones isolated from liquorice root: A comparative DFT study. *Phytochem* **2021**, *192*, 112964−112971.
(52) Attri, P.; Kim, Y. K.; Park, D. H.; Park, J. H.; Hong, Y. J.; Uhm, H. S.; Kim, K. A.; Fridman, E. H.; Choi, E. H. Generation mechanism of hydroxyl radical species and its lifetime prediction during the plasma-initiated ultraviolet (UV) photolysis. *Sci. Rep.* **2015**, *5*, 9332−9339.
(53) Zhang, H.; Andrekopoulos, C.; Joseph, J.; Crow, J.; Kalyanaraman, B. The carbonate radical anion-induced covalent aggregation of human copper, zinc superoxide dismutase, and alpha-synuclein: intermediacy of tryptophan- and tyrosine-derived oxidation products. *Free Radical Biol. Med.* **2004**, *36*, 1355−1365.
(54) Miao, Z.; Gu, X. G.; Lu, S. G.; Brusseau, M. L.; Yan, N.; Qiu, Z. F.; Sui, Q. Enhancement effects of reducing agents on the degradation of tetrachloroethene in the Fe(II)/Fe(III) catalyzed percarbonate system. *J. Hazard. Mater.* **2015**, *300*, 530−537.
(55) Song, P. P.; Sun, C. Y.; Wang, J.; Ai, S. Y.; Dong, S. J.; Sun, J.; Sun, S. Efficient removal of Cu-EDTA complexes from wastewater by

https://doi.org/10.1021/acs.est.3c00190
Environ. Sci. Technol. 2023, 57, 5034−5045

combined electrooxidation and electrocoagulation process: Performance and mechanism study. *Chemosphere* **2022**, *287*, 131971−131978.
(56) Asghar, A.; Lutze, H. V.; Tuerk, J.; Schmidt, T. C. Influence of water matrix on the degradation of organic micropollutants by ozone based processes: A review on oxidant scavenging mechanism. *J. Hazard. Mater.* **2022**, *429*, 128189−128213.
(57) Dominguez, C. M.; Oturan, N.; Romero, A.; Santos, A.; Oturan, M. A. Lindane degradation by electrooxidation process: Effect of electrode materials on oxidation and mineralization kinetics. *Water Res.* **2018**, *135*, 220−230.
(58) Yan, S. W.; Liu, Y. J.; Lian, L. S.; Li, R.; Ma, J. Z.; Zhou, H. X.; Song, W. H. Photochemical formation of carbonate radical and its reaction with dissolved organic matters. *Water Res.* **2019**, *161*, 288−296.
(59) Chen, C.; Chen, A. Q.; Huang, X. F.; Ju, R.; Li, X. C.; Wang, J.; Hao, A. M.; Zhao, M. Enhanced ozonation of Cu(II)-organic complexes and simultaneous recovery of aqueous Cu(II) by cathodic reduction. *J. Clean. Prod.* **2021**, *298*, 126837−126846.
(60) Fedorov, K.; Rayaroth, M. P.; Shah, N. S.; Boczkaj, G. Activated sodium percarbonate-ozone (SPC/O_3) hybrid hydrodynamic cavitation system for advanced oxidation processes (AOPs) of 1,4-dioxane in water. *Chem. Eng. J.* **2023**, *456*, 141027−141039.
(61) Zhang, Q.; Cheng, X. S.; Wang, W.; Fang, S. Y.; Zhang, L.; Huang, W. X.; Fang, F.; Cao, J. S.; Luo, J. Y. Unveiling the behaviors and mechanisms of percarbonate on the sludge anaerobic fermentation for volatile fatty acids production. *Sci. Total Environ.* **2022**, *838*, 156054−156063.

https://doi.org/10.1021/acs.est.3c00190
Environ. Sci. Technol. 2023, 57, 5034−5045